Procds. of the 16th Asian Regional Conference on Soil Mechanics and Geotechnical Engineering,
October 14-18, 2019, Taipei, Taiwan

Dynamic response of a double-beam system subjected to a harmonic moving load

Zhen-Dong Cui[1], P.-P. He[1], Z.-L. Zhang[1], and R.Y.S. Pak[2]

[1] State Key Laboratory for Geomechanics and Deep Underground Engineering, School of Mechanics and Civil Engineering, China University of Mining and Technology, Xuzhou, Jiangsu 221008, P. R. China.
[2] Department of Civil, Environmental & Architectural Engineering, University of Colorado at Boulder, Boulder, Colorado 80309, USA.

ABSTRACT

The governing equations are solved by the combination of Fourier transform and residue theory. The influence of the beam parameters on the dynamic response is discussed. It is shown that two cut-off frequencies and two critical velocities exist in this double-beam system. The rail has consistently higher displacement response than the slab. Load frequencies have great influence on the both beams. The Doppler Effect is significantly obvious as the load velocity exceeds critical velocities.

Keywords: double-beam; harmonic moving load; dynamic response; cut-off frequency; critical velocity

1 INTRODUCTION

A beam is a common model to characterize many moving-load problems, including tracks (Koh et al., 2003), vehicles travelling on a bridge (Lou, 2005; Lou and Zeng, 2005), high-speed aircrafts, fluids flowing in a pipe (Stein, 1970; Chen, 1972) and nano-electromechanical systems (NEMS) (Darijani et al., 2014). To model infinite beams, Euler-Bernoulli beams and Timoshenko beams are the main two physical models at present. The Euler-Bernoulli beam theory has been extensively used due to its relatively simpler mathematical formulation. The steady-state solution is necessary for a beam model subjected to a moving load. However, there are certain existing inherent difficulties involved in the mathematical formulation to solve relevant problems. Considering the effects of axial load and linear damping, Sheehan (Sheehan and Debnath, 1972) gave an analytical steady-state solution of an Euler-Bernoulli beam on an elastic foundation.

In track engineering, critical velocities are typical characteristics of a beam subjected to a moving load. Nechitailo and Lewis (2006) calculated critical velocities by utilizing analytical and finite element models. A closed-form analytical solution for critical velocities was obtained, which was based on the Euler-Bernoulli model of a beam resting on an elastic foundation regardless of damping. In some special cases, analytical solutions can be derived. Sun (2001) constructed the form of the convolution of the Green function and obtained the steady-state response of a beam on a viscoelastic foundation subjected to a harmonic line load.

This paper presents an infinite Euler-Bernoulli double-beam system resting on a viscoelastic foundation and subjected to a harmonic moving point load, including two spring-damping systems. The governing equations are solved by means of Fourier transform and residue theory. This method allows the parameters of the two beams to be completely arbitrary.

2 TRACK MODEL

The track model, referred as to a double-beam model, consists four parts: rail, rail bearing, slab and slab bearing, as shown in Fig. 1. The rail bearing connects the rail and the slab, and the slab bearing connects the slab and ground. The rail bearing and the slab bearing can be simplified as continuous spring-damping systems, and the rail and the slab can be simplified as infinite beams with different bending stiffness, respectively.

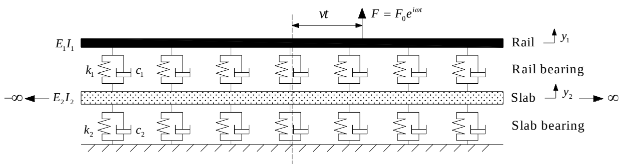

Fig. 1. Track model.

The velocity, angular frequency and amplitude of the load denote as v , ω and F_0 , respectively, and then the load can be expressed as

$$F = F_0 \cdot e^{i\omega t} \cdot \delta(x - vt) \tag{1}$$

where $\delta(x)$ is the Dirac delta function.

The governing equations of this track model are (Hussein and Hunt, 2006):

$$\left.\begin{aligned} E_1 I_1 \frac{\partial^4 y_1}{\partial x^4} + m_1 \frac{\partial^2 y_1}{\partial t^2} + k_1 (y_1 - y_2) + c_1 \left(\frac{\partial y_1}{\partial t} - \frac{\partial y_2}{\partial t}\right) = F_0 \cdot e^{i\omega t} \cdot \delta(x - vt) \\ E_2 I_2 \frac{\partial^4 y_2}{\partial x^4} + m_2 \frac{\partial^2 y_2}{\partial t^2} + k_2 y_2 - k_1 (y_1 - y_2) + c_2 \frac{\partial y_2}{\partial t} - c_1 \left(\frac{\partial y_1}{\partial t} - \frac{\partial y_2}{\partial t}\right) = 0 \end{aligned}\right\} \tag{2}$$

As the load is moving on the rail with a constant velocity, a moving coordinate system is more convenient to solve Eq. (2):

$$s = x - vt,\ w_1 = y_1,\ w_2 = y_2 \tag{3}$$

Applying the chain rule of derivation, the differentiation of Eq. (3) can be derived as

$$\left.\begin{aligned} \frac{\partial y_i}{\partial x} &= \frac{\partial w_i}{\partial s} \\ \frac{\partial^2 y_i}{\partial x^2} &= \frac{\partial^2 w_i}{\partial s^2} \\ \frac{\partial y_i}{\partial t} &= \frac{\partial w_i}{\partial t} - v\frac{\partial w_i}{\partial s} \\ \frac{\partial^2 y_i}{\partial t^2} &= \frac{\partial^2 w_i}{\partial t^2} - 2v\frac{\partial^2 w_i}{\partial s \partial t} + v^2\frac{\partial^2 w_i}{\partial s^2} \end{aligned}\right\} \tag{4}$$

where $i = 1, 2$.

The governing equations in this moving coordinate system are achieved by Eq. (3) and Eq. (4)

$$\left.\begin{aligned} & E_1 I_1 \frac{\partial^4 w_1}{\partial s^4} + m_1 v^2 \frac{\partial^2 w_1}{\partial s^2} - 2m_1 v \frac{\partial^2 w_1}{\partial s \partial t} - c_1 v(\frac{\partial w_1}{\partial s} - \frac{\partial w_2}{\partial s}) + m_1 \frac{\partial^2 w_1}{\partial t^2} \\ & + c_1(\frac{\partial w_1}{\partial t} - \frac{\partial w_2}{\partial t}) + k_1(w_1 - w_2) = F_0 e^{i\omega t}\delta(s) \\ & E_2 I_2 \frac{\partial^4 w_2}{\partial s^4} + m_2 v^2 \frac{\partial^2 w_2}{\partial s^2} - 2m_2 v \frac{\partial^2 w_2}{\partial s \partial t} - (c_1 + c_2)v\frac{\partial w_2}{\partial s} \\ & + c_1 v \frac{\partial w_1}{\partial s} + m_2 \frac{\partial^2 w_2}{\partial t^2} + (c_1 + c_2)\frac{\partial w_2}{\partial t} - c_1 \frac{\partial w_1}{\partial t} + k_2 w_2 - k_1(w_1 - w_2) = 0 \end{aligned}\right\} \tag{5}$$

The solution of Eq. (5) subjected to a harmonic point load can be assumed as

$$w_1(s,t) = \Phi(s)e^{\mathrm{i}\omega t},\quad w_2(s,t) = \Psi(s)e^{\mathrm{i}\omega t} \tag{6}$$

where $\Phi(s)$ and $\Psi(s)$ are shape functions.

According to Eq. (5) and Eq. (6), the governing equations are transformed from time-domain to frequency-domain

$$\left.\begin{aligned} & E_1 I_1 \Phi^{(4)} + m_1 v^2 \Phi'' - 2m_1 v(\mathrm{i}\omega)\Phi' - c_1 v(\Phi' - \Psi') + m_1(\mathrm{i}\omega)^2\Phi \\ & + c_1(\mathrm{i}\omega)(\Phi - \Psi) + k_1(\Phi - \Psi) = F_0\delta(s) \\ & E_2 I_2 \Psi^{(4)} + m_2 v^2 \Psi'' - 2m_2 v(\mathrm{i}\omega)\Psi' - (c_1 + c_2)v\Psi' + c_1 v\Phi' + m_2(\mathrm{i}\omega)^2\Psi \\ & + (c_1 + c_2)(\mathrm{i}\omega)\Psi - c_1(\mathrm{i}\omega)\Phi + k_2\Psi - k_1(\Phi - \Psi) = 0 \end{aligned}\right\} \tag{7}$$

Eq. (7) are ordinary differential equations and can be solved by Fourier transform

$$\tilde{F}(\xi) = \int_{-\infty}^{\infty} f(x)e^{-\mathrm{i}\xi s}dx,\quad f(x) = \frac{1}{2\pi}\int_{-\infty}^{\infty}\tilde{F}(\xi)e^{\mathrm{i}\xi s}d\xi \tag{8}$$

then Eq. (7) yields

$$\left.\begin{aligned} & [E_1 I_1 \xi^4 - m_1 v^2 \xi^2 + (2m_1 v\omega - \mathrm{i}c_1 v)\xi + (-m_1\omega^2 + \mathrm{i}c_1\omega + k_1)]\cdot W \\ & + [\mathrm{i}c_1 v\xi - (\mathrm{i}c_1\omega + k_1)]\cdot V = F_0 \\ & [\mathrm{i}c_1 v\xi - (\mathrm{i}c_1\omega + k_1)]\cdot W + \{E_2 I_2 \xi^4 - m_2 v^2\xi^2 + [2m_2 v\omega - \mathrm{i}(c_1 + c_2)v]\xi + \\ & [-m_2\omega^2 + \mathrm{i}(c_1 + c_2)\omega + (k_1 + k_2)]\}\cdot V = 0 \end{aligned}\right\} \tag{9}$$

where ξ is wavenumber.

The matrix form of Eq (9) is

$$A\begin{bmatrix} W(\xi) \\ V(\xi) \end{bmatrix} = \begin{bmatrix} F_0 \\ 0 \end{bmatrix} \tag{10}$$

where

$$A = \begin{bmatrix} a_{11} & a_{12} \\ a_{21} & a_{22} \end{bmatrix}$$
$$= \begin{bmatrix} E_1 I_1 \xi^4 - m_1 v^2 \xi^2 + (2m_1 v\omega - \mathrm{i}c_1 v)\xi + (-m_1\omega^2 + \mathrm{i}c_1\omega + k_1), & \mathrm{i}c_1 v\xi - (\mathrm{i}c_1\omega + k_1) \\ ic_1 v\xi - (\mathrm{i}c_1\omega + k_1), & E_2 I_2 \xi^4 - m_2 v^2\xi^2 + [2m_2 v\omega - \mathrm{i}(c_1 + c_2)v]\xi + [-m_2\omega^2 + \mathrm{i}(c_1 + c_2)\omega + (k_1 + k_2)] \end{bmatrix}$$

Substituting $A^{-1} = \frac{1}{|A|}\cdot\begin{bmatrix} a_{22} & -a_{12} \\ -a_{21} & a_{11} \end{bmatrix}$ to Eq. (10) yields

$$\begin{bmatrix} W(\xi) \\ V(\xi) \end{bmatrix} = A^{-1}F = \frac{1}{|A|}\cdot\begin{bmatrix} a_{22} & -a_{12} \\ -a_{21} & a_{11} \end{bmatrix}\begin{bmatrix} F_0 \\ 0 \end{bmatrix} = \frac{F_0}{|A|}\begin{bmatrix} a_{22} \\ -a_{21} \end{bmatrix} \tag{11}$$

The inverse Fourier transform can be carried out to transform Eq. (11) from ξ-domain to s-domain

$$\begin{bmatrix} \Phi(s) \\ \Psi(s) \end{bmatrix} = \frac{1}{2\pi}\int_{-\infty}^{\infty}\begin{bmatrix} W(\xi) \\ V(\xi) \end{bmatrix}\cdot e^{\mathrm{i}\xi s}d\xi \tag{12}$$

As the direct integration of Eq. (12) is complicated, residue theorem is used to solve it. The inverses of $W(\xi)$ and $V(\xi)$ have the same form, thus only $W(\xi)$ is considered in this paper

$$\Phi(s) = \frac{1}{2\pi}\int_{-\infty}^{\infty} W(\xi)\cdot e^{\mathrm{i}\xi s}d\xi \tag{13}$$

The solution of Eq. (13) is obtained by applying residue theorem, giving

$$\begin{aligned} \frac{1}{2\pi}\int_{-\infty}^{+\infty} W(\xi)e^{\mathrm{i}\xi s}d\xi &= \frac{1}{2\pi}\cdot 2\pi\mathrm{i}\cdot\sum_{j=1}^{N}\mathrm{Res}(W(\xi)e^{\mathrm{i}\xi s};\xi_j) \\ &= \mathrm{i}\cdot\sum_{j=1}^{N}\mathrm{Res}(W(\xi)e^{\mathrm{i}\xi s};\xi_j) \\ &= \mathrm{i}\cdot\sum_{j=1}^{N}\mathrm{Res}(\frac{F_0\cdot a_{22}}{|A|}e^{\mathrm{i}\xi s};\xi_j) \end{aligned} \tag{14}$$

where N is the number of singular points of $\frac{F_0\cdot a_{22}}{|A|}e^{i\xi s}$; ξ_j is the jth singular point.

The singular points can be calculated by $|A| = 0$. According to Eq. (10), $|A|$ is an eight polynomial, thus if $v \neq 0$, there are eight complex roots in the complex field.

3 RESULTS AND ANALYSIS OF AN EXAMPLE

The parameters of the four parts are listed in Table 1.

Table 1. Parameters of a double-beam system.

Rail	Slab
$E_1 I_1 = 1.33\times10^7\,\mathrm{N\cdot m^2}$	$E_2 I_2 = 6\times10^7\,\mathrm{N\cdot m^2}$
$m_1 = 60\mathrm{kg/m}$	$m_2 = 1333\mathrm{kg/m}$
$k_1 = 40\times10^6\,\mathrm{N/m^2}$	$k_2 = 50\times10^6\,\mathrm{N/m^2}$
$c_1 = 6\times10^3\,\mathrm{N/m/(m/s)}$	$c_2 = 40\times10^3\,\mathrm{N/m/(m/s)}$

3.1 Dispersion curve and cut-off frequency

$|A|$ is a function of wavenumber ξ, angular frequency ω ($\omega = 2\pi f$) and load velocity v.

Dispersion curve denotes the relationship between frequency and wavenumber. When $v=0$, cut-off frequencies of the double-beam can be obtained. When the load frequency approaches the cut-off frequency f_c at $v=0$, the displacements of the two beams at loading point ($s=x-vt=0$) reach the maximum value. The dispersion curve at $v=0$ is shown in Fig. 2.

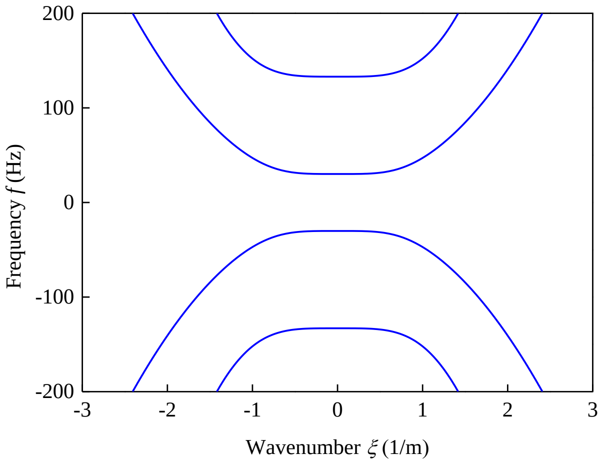

Fig. 2. Dispersion curve at v=0.

As shown in Fig. 2, the dispersion curve is symmetrical with respect to $\xi=0$ and $f=0$. The two cut-off frequencies correspond to the positive frequencies at $\xi=0$, that is, $f_1=30.12\text{Hz}$ and $f_2=133.00\text{Hz}$. Considering a single slab beam, its cut-off frequency is $f_{\text{slab}}=\frac{1}{2\pi}\sqrt{\frac{k_2}{m_2}}=30.82\text{Hz}$, which is close to the first cut-off frequency f_1. And similarly, the cut-off frequency of a single rail beam can be calculated as $f_{\text{rail}}=\frac{1}{2\pi}\sqrt{\frac{k_1}{m_1}}=129.95\text{Hz}$, which approaches to the second cut-off frequency f_2. The results show that the lower cut-off frequency is controlled by the slab with higher bending stiffness and the higher cut-off frequency is determined by the rail with lower bending stiffness.

3.2 Critical velocity

When the load frequency $f=0$, the dynamic response of the double-beam experiences the maximum at $v=v_c$. Fig. 3 shows the relationship between displacements and velocities at $f=0$. As can be seen from Fig. 3, this double-beam system has two critical velocities: $v_{c1}=284\text{m/s}$ and $v_{c2}=860\text{m/s}$. The displacements decrease to be almost zero when load velocity exceeds 1000m/s. As described previously, the rail has considerably higher displacements than the slab at any load velocity. The displacements of the rail at the second critical velocity are higher than those at the first critical velocity, while the displacements of the slab at the second critical velocity are minimal.

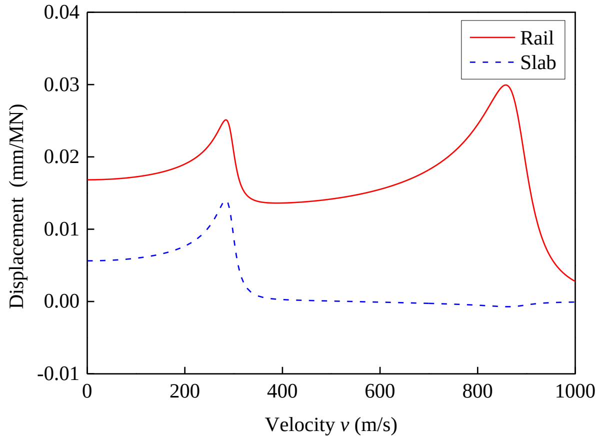

Fig. 3. Variations of displacements with load velocity at f=0 and s=0.

3.3 Variations of the load frequency

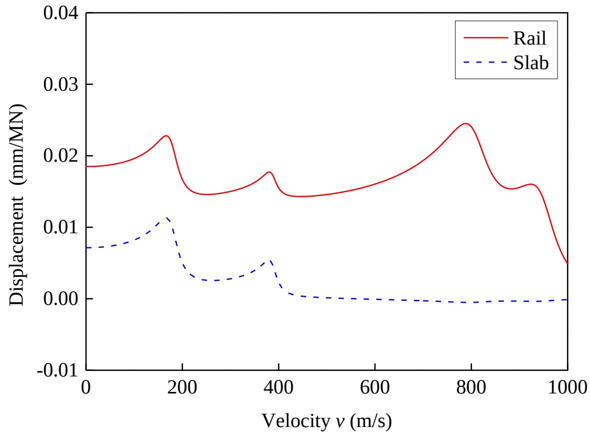

(a) f=15 Hz

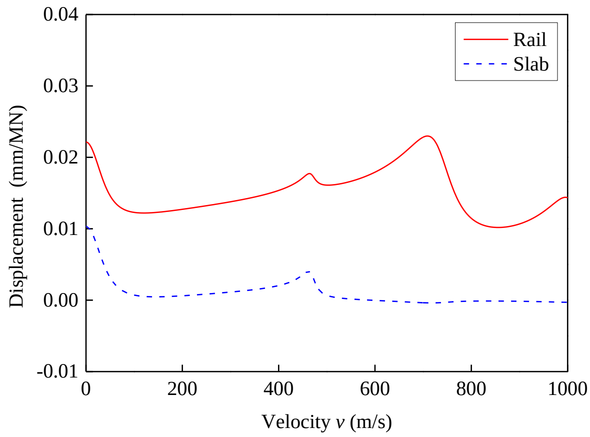

(b) f=30 Hz

Fig. 4. Variations of displacements with load velocity.

Fig. 4 illustrates the variations of the displacements with respect to velocity at different load frequencies. As shown in Fig.3 and Figs. 4(a), (b), the peak displacements move left with the load frequency approaching to the first cut-off frequency. And when the load frequency ($f=30\text{Hz}$) is near the first cut-off frequency, the maximum displacement corresponds to $v = 0$, which accords with the definition of cut-off frequency in previous section. When the load frequency is between the first cut-off frequency and the second cut-off frequency, the velocities corresponding to peak displacements decreases again, which is similar to the trend when the load frequency exceeds the first cut-off frequency. Therefore, an actual load which contains frequencies that are near cut-off frequencies can lead to a great displacement.

3 CONCLUSION

In this paper, an infinite Euler-Bernoulli double-beam system resting on a viscoelastic foundation and subjected to a harmonic moving point load is investigated and parametric study is carried out. The governing equations are solved by utilizing Fourier transform and residual theory. Numerical results of an example are presented and then cut-off frequencies and critical velocities are calculated.

It is concluded that two cut-off frequencies and two critical velocities exist in this double-beam system. The rail has consistently higher displacement response than the slab. Load frequencies and velocities have great influence on the both beams. Displacements tend to be stable with respect to load velocities at high load frequency.

ACKNOWLEDGEMENTS

This work presented in this paper was supported by National Key Research and Development Program (Grant No. 2017YFC1500702).

REFERENCES

Koh, C.G., Ong, J.S.Y., Chua, D.K.H., Feng, J. (2003). Moving element method for train-track dynamics. Int J Numer Methods in Eng, 56(11): 1549-1567.

Lou, P. (2005). Vertical dynamic responses of a simply supported bridge subjected to a moving train with two-wheelset vehicles using modal analysis method. Int J Numer Methods in Eng, 64(9): 1207-1235.

Lou P., Zeng Q. (2005). Formulation of equations of motion of finite element form for vehicle-track-bridge interaction system with two types of vehicle model. Int J Numer Methods in Eng, 62(3): 435-474.

Stein, R.A., Tobriner, M.W. (1970) Vibration of pipes containing flowing fluids. J Appl Mech, 37(4): 906-916.

Chen, S. (1972). Vibration and stability of a uniformly curved tube conveying fluid. J Acoust Society America, 51(1B): 223-232.

Darijani, H., Mohammadabadi, H. (2014). A new deformation beam theory for static and dynamic analysis of microbeams. International Int J Mech Sci, 89: 31-39.

Sheehan, J.P., Debnath, L. (1972). On the dynamic response of an infinite Bernoulli-Euler beam. Pure Appl Geophys, 97(1): 100-110.

Nechitailo, N.V., Lewis, K.B. (2006). Critical velocity for rails in hypervelocity launchers. Int J Impact Eng, 33(1): 485-495.

Sun, L. (2001). A closed-form solution of a Bernoulli-Euler beam on a viscoelastic foundation under harmonic line loads. J Sound Vib 2001; 242(4): 619-627.

Hussein, M.F.M., Hunt, H.E.M. (2006) Modelling of floating-slab tracks with continuous slabs under oscillating moving loads. J Sound Vib 2006; 297(1): 37-54.